Fine Structure of the Solar Wind Turbulence Inferred from Simultaneous Radio Occultation Observations at Widely-Spaced Ground Stations

M.K. Bird*, P. Janardhan†, A.I. Efimov, L.N. Samoznaev, V.E. Andreev**, I.V. Chashei‡ and P. Edenhofer, D. Plettemeier, R. Wohlmuth§

*Radioastronomisches Institut, Universität Bonn, 53121 Bonn, Germany
†Astronomy & Astrophysics Division, Physical Research Laboratory, Ahmedabad, 380 009, India
**Inst. for Radio Engineering & Electronics, Russian Academy of Science, Moscow, 101999, Russia
‡Lebedev Physical Institute, Russian Academy of Science, Moscow, 117924, Russia
§Institut für HF-Technik, Universität Bochum, 44780 Bochum, Germany

Abstract. Coronal radio sounding experiments with the Ulysses spacecraft at superior conjunction provided numerous opportunities for simultaneous observations of the downlink signals at two widely-spaced ground stations. In some instances the duration of these observations extended for up to four hours, thereby allowing studies of solar wind turbulence dynamics at spatial scales comparable with the corona-projected distance between ground stations (a few thousand km). The frequency and phase fluctuations produced by electron density inhomogeneities are normally quite well correlated on these scales. The spectral index of the temporal frequency fluctuation spectra varied over a wide range during the observations. The cross-correlation coefficient reached maximal values (≈ 0.5) when the spectral index was high (≈ 1), but no correlation could be detected when the spectral index became small (< 0.4). Similar behavior in many of the data sets implies that this is a common, if not permanent, feature of the solar wind. Possible reasons for the fluctuation decorrelation are analysed. The decorrelation at heliocentric distances ≈ 10 $R_\odot$ most likely results from continual deformation of the solar wind density irregularities during their motion across the radio ray paths.

INTRODUCTION

Coronal sounding observations of occulted radio signal parameters such as fluctuations of amplitude, phase, frequency or Faraday rotation at two or more separated ground stations is an effective method to study solar wind motion, especially in those regions inaccessible to *in situ* measurements. A general assumption underlying these observations is that the modulating irregularities are convected with a speed approximately equal to the bulk velocity of the solar wind. Strictly speaking, this assumption is valid only at large heliocentric distances where the solar wind is superalfvenic and supersonic. For sufficiently accurate measurements of correlation time delay, the spacing between the ray paths to each ground station should not be much less than the typical spatial scale of the measured fluctuations. This is the diffraction (Fresnel) scale ($\simeq 100$ km) in the case of amplitude (intensity) fluctuations (Armstrong and Coles, 1972; Coles and Kaufman, 1978), and the dominant energy containing scale in the electron density spatial power spectrum in the case of the other fluctuating parameters. On the other hand, the spacing between antennas should not be too much larger than the typical scale of the irregularities in order to avoid degradation of the cross correlation.

In contrast to phase or Faraday rotation fluctuations, frequency fluctuation observations produce a flatter temporal power spectrum (Armand et al., 1987; Wohlmuth et al., 2001) that enables use of smaller spacings between ray paths and, consequently, between ground-based antennas. Another important aspect of spaced observations is the length of the fluctuation record. Whereas a long observation time is needed to reduce statistical errors, the actually attainable interval length is always limited under real experimental conditions. Some typical features of spaced frequency fluctuation observations are studied in this paper using measurements obtained as part of the Ulysses Solar Corona Experiment (SCE) during that spacecraft's solar conjunctions at the large tracking antennas of the NASA Deep Space Network (DSN). Results similar to those presented below were found in other two-station observations with the Galileo spacecraft. Emphasis is placed here on the dependence of the cross correlation on the spatial spectrum of density irregulatities at heliocentric (solar offset) distances near 10 $R_\odot$. Earlier indications for the existence of such a de-

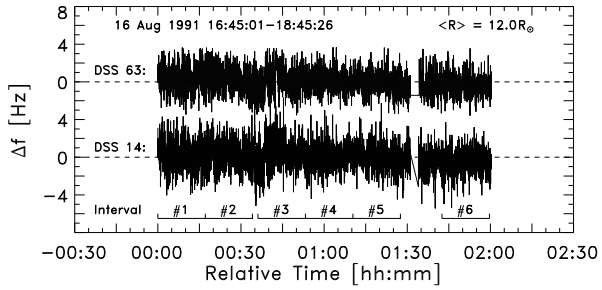

FIGURE 1. *Ulysses frequency residual records on 16 August 1991 at the ground stations Madrid (DSS 63) and Goldstone (DSS 14), divided into 6 subintervals.*

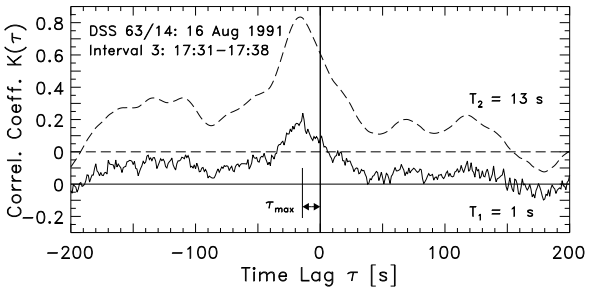

FIGURE 2. *Frequency fluctuation cross-correlation functions for Interval 3 with $< \alpha_f > = 1.015$. Lower curve: raw data before filtration; upper curve: after filtration (curve and scale displaced upward by 0.2).*

pendence were reported by Armand and Efimov (1984).

OBSERVATIONS AND DATA PROCESSING

Records of the Ulysses (Doppler) frequency residuals (carrier frequency: 2.295 GHz) at the two DSN ground stations Madrid (DSS 63) and Goldstone (DSS 14) are presented in Fig. 1. The frequency residuals were recorded at a sampling rate of 1 s^{-1}. The mean heliocentric distance and heliographic latitude of the solar proximate points along the ray paths were $\langle R \rangle$ = 12.0 $R_\odot$ and $\langle \phi \rangle$ = 18.7°, respectively. The ground baseline projection in the corona for the combination Madrid/Goldstone is closer to the radial direction than the projections of the other possible ground station pairs.

The records for the two ground stations in Fig. 1 are qualitatively very similar. The two-hour records shown in Fig. 1 were divided into 6 subintervals, each of 1024 s duration. Temporal power spectra and cross-correlation functions were calculated for each interval and the results are summarized in Table 1.

The following are listed in Table 1 from top to bottom:

- UT start and end time for the intervals 1-6
- heliocentric distance of ray path proximate point: R
- coronal separation of ray path proximate points: ΔS
- the radial projection of $\Delta\vec{S}$: ΔR
- RMS frequency fluctuations at DSS 14: σ_{f14}
- RMS frequency fluctuations at DSS 63: σ_{f63}
- spectral power exponent at DSS 14: α_{f14}
- spectral power exponent at DSS 63: α_{f63}
- $\langle \alpha_f \rangle = (\alpha_{f14} + \alpha_{f63})/2$

The last rows of Table 1 contain the following quantities for the raw data (effective filtration time T_1 = 1 s) and filtered data (T_2 = 13 s):

- maximum cross-correlation time lag: $\tau_{\max}$
- maximum value of the temporal cross-correlation function: $K_{\max} = K(\tau_{\max})$
- estimated solar wind speed: $v_c = \Delta R/\tau_{\max}$.

A comparison of the data measured separately at DSS 14 and DSS 63 demonstrates their close similarity for both stations. The values of σ_f differ by no more than 15%, and the values of α_f differ by no more than 25% for all intervals listed in Table 1. These variations are only marginally higher than the formal errors (∼10%) associated with the determination of these quantities. At the same time, the spectral parameters vary considerably from one interval to another, i.e., the typical scale of temporal variations is of the order of 20 minutes.

The strength of the cross correlation was found to be particularly variable. The maximum cross-correlation coefficient $K_{\max}$ for the raw data (T_1 = 1 s) varies from the rather high value of 0.42 for Interval 3 down to indistinguishable values for the Intervals 4-6. In order to increase the accuracy of the time lag derived from the cross-correlation functions (see Table 1), the records of Fig. 1 were passed through a high-frequency (low-pass) filter. The cross-correlation data before (effective filtration time $T_1 = 1s$) and after the filtration procedure ($T_2 = 13s$) can be compared in Table 1. Removal of the high-frequency fluctuations produces a considerable increase in the cross-correlation level as well as the appearance of a detectable time lag near the expected numerical value.

CROSS CORRELATIONS BETWEEN SPACED FREQUENCY FLUCTUATIONS

The increase in the cross-correlation level following the filtration procedure is shown graphically in Figs. 2-4.

TABLE 1. Results of frequency fluctuation measurements at Goldstone (DSS 14) and Madrid (DSS 63)

Interval	#1	#2	#3	#4	#5	#6
UT	16:45-17:02	17:02-17:19	17:21-17:38	17:38-17:55	17:55-18:12	18:27-18:44
R [$R_\odot$]	12.10	12.07	12.04	12.01	11.98	11.92
ΔS [km]	6555	6447	6295	6143	5981	5471
ΔR [km]	6533	6415	6249	6083	5905	5344
σ_{f14} [Hz]	1.28	1.06	1.02	0.90	0.96	1.02
σ_{f63} [Hz]	1.19	1.02	1.13	0.92	0.81	0.93
α_{f14}	0.58	0.57	1.06	0.37	0.30	0.25
α_{f63}	0.66	0.43	0.97	0.36	0.39	0.28
$\langle\alpha_f\rangle$	0.62±0.07	0.50±0.06	1.02±0.08	0.37	0.35	0.26
unfiltered data [T_1 = 1 s]						
$\tau_{\max 1}$ [s]	-18.8±2.2	-14.1±1.4	-14.3±1.3	-	-	-
$K_{\max 1}$	0.21±0.02	0.15±0.09	0.42±0.09	-	0.06	-
v_{c1} [km s^{-1}]	348±41	455±45	437±40	-	-	-
filtered data [T_2 = 13 s]						
$\tau_{\max 2}$ [s]	-15.5±1.1	-15.2±0.8	-16.1±0.7	-14.3	-12.4	-
$K_{\max 2}$	0.63±0.03	0.60±0.09	0.84±0.10	0.33	0.41	-
v_{c2} [km s^{-1}]	421±30	422±22	388±17	425	476	-

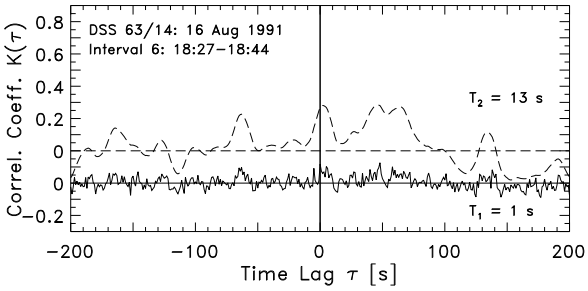

FIGURE 3. *Frequency fluctuation cross-correlation functions for Interval 6 with $<\alpha_f>$ = 0.264 (curves as in Fig. 2).*

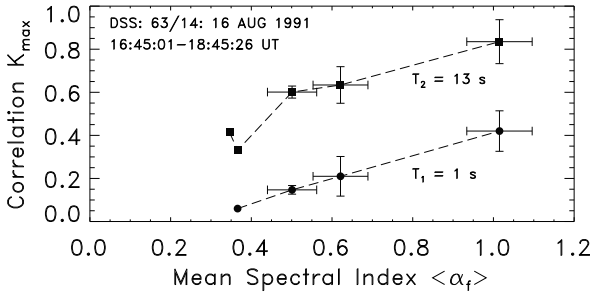

FIGURE 5. *Cross-correlation coefficient $K_{\max}$ versus power exponent $\langle\alpha_f\rangle$ before (circles) and after (squares) filtration.*

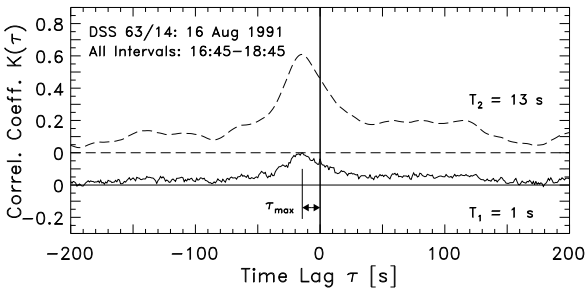

FIGURE 4. *Frequency fluctuation cross-correlation functions for the entire record in Fig. 1 (curves as in Fig. 2).*

The data of Table 1 also indicate that the maximum cross correlation of the frequency fluctuations $K_{\max}$ increases with the index of the fluctuation power spectrum $\langle\alpha_f\rangle$. This approximately linear dependence is shown in Fig. 5 for both filtered and unfiltered data.

In order to explain the behavior in Fig. 5 qualitatively, we briefly consider possible causes of decorrelation between temporal fluctuations measured simultaneously at spaced sites. The principle candidates relevant to our observations are the following:

- Motion of the irregularities transverse to the coronal projection of the ground baseline
- Solar wind velocity spread connected with the presence of streams with different speeds in the modulated propagation medium (Chashei et al., 2000);
- Growth of irregularities during their motion between the radio ray paths, the so-called "bubbling pattern" (Little and Ekers, 1971).

For all three above cases, it can be shown that the maximum cross correlation of fluctuations registered at spaced sites will increase upon decreasing the ratio "site spacing / spatial correlation size". The first possible cause above is most probably not responsible for the

dependence of Fig. 5, because the angle between the coronal projection of the baseline and the radial direction is quite small (see Table 1). Furthermore, the expected value of the ratio between the instanteneous convection velocity spread and the mean solar wind speed at small heliocentric distances should not be greater than at large distances where this ratio is much less than unity (Chashei et al., 2000). For the last possible cause, random changes of moving irregularities can be characterized by a chaotic velocity w_{ch}. Using spaced interplanetary scintillation observations, Ekers and Little (1971) found that the chaotic velocity is comparable to the solar wind speed ($w_{ch} \gtrsim v_c$) at heliocentric distances less than 10 $R_\odot$, i.e., in that region appropriate to the observations presented in this paper. The increase in the cross correlation with increasing spectral power exponent is thus explained naturally by a corresponding increase in the spatial turbulence correlation scale.

Moreover, weak cross correlation for the flat temporal fluctuation spectra indicates that the typical "lifetime" of the irregularities at a given scale L is comparable to the convection time L/v_c. Consequently, since $w_{ch} \gtrsim v_c$, the cross correlation is dominated by irregularities with scales $L \gtrsim \Delta R$, where ΔR is the radial coronal projection of the radio ray path separation. The increase in cross correlation resulting from high-frequency filtration evidently has the same explanation.

CONCLUSIONS

A statistical analysis of frequency fluctuations recorded during coronal radio sounding experiments with the Ulysses and Galileo spacecraft shows a high degree of similarity between the power spectral parameters measured simultaneously at widely-spaced ground stations with short-time averaging. However, considerable temporal variations of the spectral parameters, particularly the power exponent, were detected on typical time scales of about 20 min.

The cross-correlation coefficient of frequency fluctuations at spaced ground stations was also found to be quite variable from one 20-minute interval to the next. The cross-correlation level $K_{\max}$ was found to increase roughly linearly with increasing spectral power exponent. Whereas no cross-correlation time lag could be determined at high sampling rate for the case of flat temporal spectra ($\alpha_f < 0.4$), $K_{\max}$ reached sufficiently high levels $\simeq 0.5$ for the case of steep spectra ($\alpha_f \geq 1$).

High-frequency filtration of the initial records results in an even steeper increase of $K_{\max}$. The dependence of $K_{\max}$ on α_f and the filtration effect show that those solar wind density irregularities with scales less than the radial projection of the baseline spacing do not produce correlated frequency fluctuations. The decorrelation of fast frequency fluctuations is best explained for the range of heliocentric distances near 10 $R_\odot$ by the temporal changes of density irregularities during their convection between the separated radio ray paths to the ground stations. The typical time scale for these changes in the irregularities is greater than, but comparable with the convection time. The conclusions of Ekers and Little (1971) on fast changes of irregularities with scales $\lesssim$ 100 km is thus extended here to the range of irregularities of size 10^3 – 10^4 km. The possible cause of this frequency fluctuation bubbling is most likely associated with the propagation and damping of wave-like density irregularities (Chashei et al., 2000).

ACKNOWLEDGMENTS

This work presents results of a bi-national research project partially funded by the Deutsche Forschungsgemeinschaft (DFG) and by the Russian Foundation for Basic Research (RFBR), Grant 00-02-04022. Additional support from the RFBR, Grant 00-02-17845, and from the Russian Ministry of Industry, Technology and Science, is acknowledged.

REFERENCES

1. Armand, N.A., Efimov, A.I., 1984, Correlation of frequency fluctuations of waves propagating in turbulent media, *Radiotechn. Electron. 29*, 1649-1657.
2. Armand, N.A., Efimov, A.I., Yakovlev O.I., 1987, A model of solar wind turbulence from radio occultation experiments, *Astron. Astrophys. 183*, 135-141.
3. Armstrong, J.W., Coles, W.A., 1972, Analysis of three-station interplanetary scintillation, *J. Geophys. Res. 77*, 4602-4610.
4. Chashei, I.V., Shishov, V.I., Kojima, M., Misawa, H., 2000, Velocity fluctuations in the interplanetary scintillation pattern, *J. Geophys. Res. 105*, 27409-27417.
5. Coles, W.A., Kaufman, J.J., 1978, Solar wind velocity estimations from multi-station interplanetary scintillation, *J. Geophys. Res. 83*, 1413-1420.
6. Ekers, R.D., Little, L.T., 1971, The motion of the solar wind close to the Sun, *Astron. Astrophys. 10*, 310-316.
7. Little, L.T., Ekers, R.D., 1971, A method for analyzing drifting random patterns in astronomy and geophysics, *Astron. Astrophys. 10*, 306-309.
8. Wohlmuth, R., Plettemeier, D., Edenhofer, P, Bird, M.K., Efimov, A.I, Andreev, V.E., Samoznaev, L.N., Chashei, I.V., 2001, Radio frequency fluctuation spectra during the solar conjunctions of the Ulysses and Galileo spacecraft, *Space Sci. Rev. 97*, 9-12.